PREPRINT OF:
Generation of Runaway Electron Beams and X-Rays in High Pressure Gases, Volume 1: Techniques and Measurements
Chapter 8

Chapter

X-RAYS FROM LONG LABORATORY SPARKS IN AIR

Joan Montanyà[1,*], Víctor March[2,†] and Pavlo Kochkin[3,‡]
[1]Electrical Engineering Department,
Universitat Politècnica de Catalunya, Terrassa, Barcelona, Spain
[2]Gamesa Innovation and Technology S.L., Sarriguren, Spain
[3]Birkeland Centre for Space Science,
University of Bergen, Bergen, Norway

ABSTRACT

Researchers of laboratory experiments with long sparks found a tool to investigate the mechanisms of lightning in nature. These include the recent discovery of the Terrestrial Gamma-ray Flashes detected from space and the X-rays from lighting leaders at ground. For more than ten years, researchers have been investigating the origin of X-rays in laboratory discharges and speculated on the resemblances with lightning. In this chapter, we provide an overview of the experimentation with energetic emissions from long sparks.

1. INTRODUCTION

Long sparks in air at laboratory scale are probably the closest electric discharges to the majestuous lightning in the Earth's atmosphere. For many decades, high voltage laboratory experiments helped scientists to understand the nature of streamers and leaders in electric discharges and their resemblances to lightning. In nature, lightning is supposed to be the source of the flux of high-energetic photons to space named Terrestrial Gamma ray Flashes (TGFs). After twenty years of the discovery of TGFs by Fishman et al. (1994), the source of such intense emissions is still controversial. More recently, at ground, Moore et al. (2001) found bursts of X-rays coming from lightning negative leaders progressing to ground before the return stroke. These emissions seem to be related with negative leader steps. It is still unclear whether and how

* Email: montanya@ee.upc.edu.
† Email: vmarch@gamesacorp.com.
‡ Email: pavlo.kochkin@uib.no.

these emissions at ground level and those detected from space are related. It was only a little more than ten years ago when X-rays were also found in high voltage laboratory long sparks by Dwyer et al. (2005). This finding inspired researchers to investigate the processes of electrical discharges including lightning that lead to emitting high energy radiation in the controlled conditions of a laboratory. Research has brought scientists to attribute the generation of runaway electrons in lightning and laboratory experiments to be related with the large electric fields that can be present at leader tips and streamers.

In the recent history of this type of experiment, two periods can be distinguished. During the first period, from 2005 to 2009, the tests were focused on finding the conditions of the production of X-rays. It was found that negative sparks are more efficient, producing high-energy emissions. These emissions were found to come from the spark-gap and to occur near before the peak of the voltage and the breakdown of the gap. At this time, Cooray et al. (2009) suggested that the emissions might be related to the encounter of negative and positive streamer before the breakdown of the spark-gap. In the second period, from 2010-present, the experiments have been focused to study the influence of the voltage rise time, the identification of the discharge process related to the X-ray emissions and the relation with microwave electromagnetic radiation. In this period, March and Montanyà (2010) showed the influence of the voltage growth on the detection rates. They found that fast rise time impulses are more efficient producing X-rays, probably because higher electric fields can be present at the gap or because the fast energy gains of electrons. That is similar to the 'overvoltage' concept in short nanosecond sparks (e.g., Babich and Loiko 2010 and references therein) where fast rise time impulses allow applying higher voltages to a spark-gap. On the other hand, by means of ultra-high speed single frame intensified cameras, Kochking et al. (2012) observed that X-rays are produced in the encounter of positive and negative streamers. In positive discharges, the emissions have been related to the encounter of positive and negative streamers, so the presence of negative streamers is a necessary condition. In this case, X-rays correlate with the encounter of positive streamers from the anode (positive high voltage electrode) with negative streamers from the cathode (grounded electrode). Negative sparks are more complex, in that case X-rays have been also related to the encounter of positive and negative polarities. Nevertheless, the encounters are due to bidirectional streamer development near the cathode pre-treated by previous streamer bursts. Finally, peaks of microwave radiation have been recently found to coincide with the detection of X-rays in long laboratory sparks. According to the current acknowledge, the peak of radiation would be related to the encounter of streamers but the mechanism of emission is still not precisely defined.

In this chapter, we introduce the reader to the basic experimental high voltage setup and techniques for investigating X-ray emissions on long sparks. The development of a discharge in an inhomogeneous gap and fast varying voltage is very complex. The recent use of state-of-the-art digital cameras allows characterizing the development of streamers and leaders in time. That is very important because X-rays are produced in a very particular time of a discharge. The development of discharge in a meter and microsecond scale is reviewed. Next, the occurrence of X-rays in high voltage impulses is presented and the previous experiments are summarized. Two particular sections are dedicated to the occurrence of X-rays in negative and positive discharges. The effects of the applied voltage, the gap configuration, polarity asymmetry and microwave emissions are presented in individual sections.

2. LABORATORY SETUP

The minimum equipment requiered for investigating energetic radiation from long sparks comprises a high voltage generator to generate impulses at the MV range, a capacitive voltage divider to measure the applied voltage to the spark-gap and one or more detectors in order to detect high energy emissions (Figure 1). To have a wider picture of the processes that might be related with the occurrence of energetic radiation, during the recent years some additional instruments have been incorporated to the experiments. On one hand, optical instruments provide a very useful information for understanding the development of long sparks. The most popular instruments are digital UV sensitive photo cameras and ultra high-speed ns exposure cameras. Photometers are a more economical alternative used in laboratories. On the other hand, currents at the electrodes can be measured as well as electromagnetic radio emissions especially at the range of microwaves.

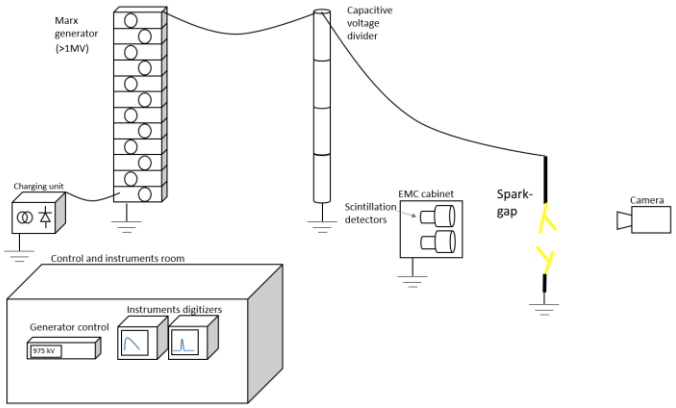

Figure 1. Minimum high voltage laboratory setup for investigating high-energy emissions from long sparks.

2.1. High Voltage Impulse Generator

The experimentalist can find impulse generators in most of the high voltage laboratories devoted to testing electrical insulation of devices or components as well lightning protection systems. Most of the countries have large high voltage generators at national laboratories but also some private companies, universities and research institutes. The most common generator able to produce very high voltages is the Marx Generator (Marx 1924).

In the generator depicted in Figure 2, very high voltages are achieved by charging several (N) capacitors (C_g) in parallel and then discharging them in series. Each capacitor forms a stage and it is charged at a certain DC voltage (U_o) by means of a DC power supply and the charging resistors R_C. The output voltage will result as the addition of the individual stage voltages. The series connection of the stages is achieved by means of triggering the switching spark-gaps (S).

After all stages are connected in the series, the capacitors will be discharged. In order to adjust the decay-time of the desired output voltage, the discharge of the capacitors is produced through the resistors R_C, which are connected in parallel with each individual stage. In series with the output of the generator, the damping resistors R_S lead to adjust the rise-time of the voltage impulse. Typical voltage impulses are the standardized lightning impulse (rise/fall time: 1.2/50 µs) and the switching impulse (250/2500 µs). Researchers found the use of the standard lightning impulse to be adequate for the production of high-energy radiation. March and Montanyà (2010) discussed the effect of the voltage growth in relation to the efficiency of producing X-rays. The steepness and the peak of the output voltage depend on the capacitances connected in parallel with the generator. One capacitance to consider is the capacitive voltage divider (C_{VD}, ~500-1000 pF) used to measure the output voltage. Another capacitance is the spark-gap electrodes capacitance (C_{SD}) where it is typically very low (up to few pF). The inductances of the generator, and especially the inductances due to the loop formed at the output of the generator, contribute to limit the minimum voltage rise time.

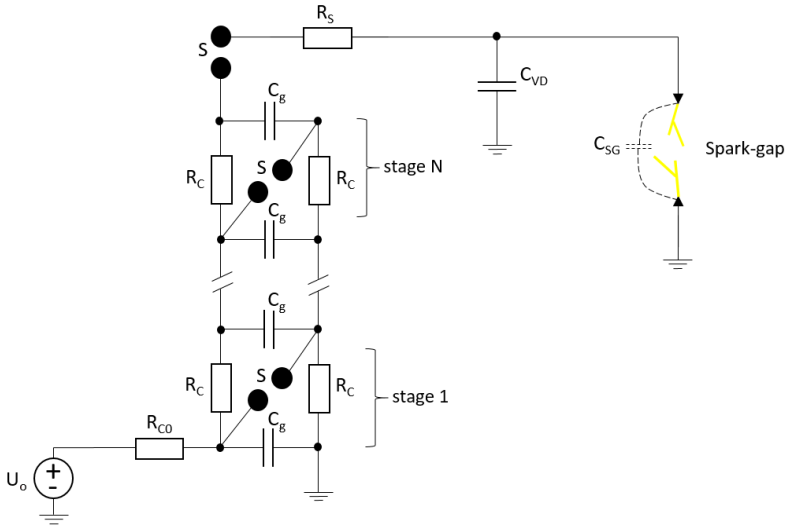

Figure 2. Basic schematic of a Marx generator of N stages.

In the setup in Figures 1 and 2, the measured voltage is done by means of the capacitive divider. Nevertheless, the voltage at the divider is not exactly the voltage at the spark gap because the inductance of the formed by the loop between the voltage divider and the gap. A meticoulous researcher shall find the best arrangement for obtaining the most close spark-gap voltage measurement.

2.2. Spark-Gaps

In experiments with short gaps, energetic electrons might emit X-rays due to Bremsstrahlung when they collide with components of the experiment itself. Moreover, in short gaps the corona/streamer discharge bridges the gap very fast. One of the purposes of investigating with long sparks is to represent similar conditions that might be present in the tips of lightning leaders in nature and to favor the production of X-rays by collisions with air molecules.

The spark-gap is designed in such way that the voltage applied will produce a very disturbed electric field that will lead to the initiation of a discharge. Typical electrode arrangements are rod-to-rod, sphere-to-sphere, rod-to-plane and the cone-shaped electrodes. At the electrodes, currents can be measured by means of current shunts or rogowski coils. The measurement of currents at grounded electrodes is more trivial than in the high voltage side because of the insulation and EMI requirements of the signals. Fiber optic converters are used to transport safe and clean measured signals at the spark-gap to the oscilloscopes at the control and instruments room.

Researchers have been investigating the properties of positive and negative sparks. This polarity convention refers to the polarity of the high voltage electrode with respect to the grounded electrode. Nevertheless, that does not means that during the discharge coronas, streamers or leaders of both electric charge polarity can be present in the gap. For each polarity, the type of electrodes has a different effect on the inception and development of the discharge. As an example, a gap formed by a plate high voltage electrode and a rod ground electrode with negative polarity, the positive streamer or leader from the grounded electrode can dominate the discharge.

2.3. Detectors

Detection of X-ray photons in high voltage experiments with long gaps has been achieved by means of scintillation detectors. These detectors are typically the coupling of a scintillator with a light detector such as a photomultiplier tube (PMT). The scintillator is a material that reemits the absorbed energy from a passing particle in the form of light. That is the case of the common used NaI(Tl) and $LaBr_3$(Ce) scintillators where the incidence of energetic photons results in the production of light. In a detector, the produced light is detected by a PMT converting it to electrons and multiplied resulting in an electrical pulse. This electrical pulse is recorded by means of an oscilloscope. Using oscilloscopes with multiple channels, signals form several detectors that can be conveniently combined with other signals of the experiment such as voltage and currents.

Detectors based on NaI(Tl) scintillators have been widely used because relatively large crystals can be produced inexpensively compared to $LaBr_3$(Ce) scintillators. The thickness of the scintillator is related to the absorption efficiency for each energy whereas the area affects the probability of detection (efficiency). Other metrics of a detector very important for experiments with long sparks are the rise and decay time constants. NaI(Tl) scintillators have a typical rise time of ~25 ns and a decay time of ~250 ns contrasting with the fast ~10 ns and ~25 ns rise and decay times, respectively of a $LaBr_3$(Ce) detector. In high voltage experiments

X-rays are produced during a very narrow interval of time in the range of few ns. The time resolution $LaBr_3$(Ce) makes it better to distinguish individual emissions but even the fast response of the detector pile-up can be produced (e.g., Kochkin 2014). Another remarkable characteristic of $LaBr_3$(Ce) detectors is the better energy resolution compared to NaI(Tl) detectors. The two drawbacks of the $LaBr_3$(Ce) detectors are the low-energy response (e.g., Dorenbos 2004) and the internal radioactivity.

Figure 3 plots a typical arrangement of an X-ray detector for high voltage experiments. The detector is placed in an EMC cabinet in order to reduce the intense electromagnetic interference (EMI) produced by the generation of the high voltage impulse and the occurrence of the discharge. The detector is commercially available as a unit comprising the scintillator crystal and the PMT with the corresponding housing of the crystal, couplings and magnetic shielding of the PMT. In some detectors, the electronics for adapting the output of the PMT to the suitable signal for an oscilloscope (preamplifier) and the high voltage (HV) power supply input are in the form of a plug-in socket. Pulse shaping electronics are not used for experiments when the purpose is the characterization of individual pulses as occurs in long sparks. In the high voltage laboratory the detector is placed not far from the spark-gap whereas the oscilloscopes are outside of the high voltage room. In order to minimize the interferences it is recommended to use internal batteries as energy source for the detector and provide the output signal to the oscilloscopes by means of fiber optic links.

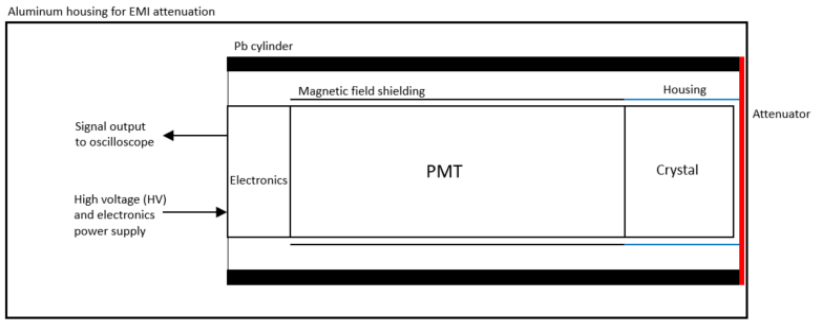

Figure 3. Typical scintillator detector arrangement for X-ray detection in high voltage experiments.

Before setting up the detector at the high voltage room of the laboratory, it needs to be calibrated. The calibration is recommended to include all the components from the detector including the housings, attenuators, cables, and power supplies up to the registration oscilloscopes. The output of the detector is calibrated at different energies and the linearity is obtained. Common radioactive sources used as reference for calibration with their emitted energies are: ^{241}Am (59.5 keV), ^{137}Cs (622 keV) and ^{60}Co (1.25 MeV). It is important to determine de attenuation due to the EMC housing (typically few tens of keV) and the attenuators installed on purpose (e.g., Pb of thickness of few cm causes the absorption in the MeV).

Finally, as indicated above, when interpreting the signals from the detector one must take into account the pile-up effect where simultaneously registered lesser energy photons cannot

be distinguished from intense individual photons and are added. In the high voltage lab, as a rule of thumb the maximum energy that single electrons can gain is limited by the maximum applied voltage to the gap.

3. DEVELOPMENT OF METER AND MICROSECOND SCALE SPARKS

Before addressing the occurrence of X-ray emissions in long sparks, in this section we will show how a meter-scale discharge develops from its first light emission till the final breakdown. The images were obtained at High-Voltage Laboratory of Eindhoven University of Technology. A 2 MV Haefly Marx generator was available in the laboratory up to 2014 and is currently dismantled. The setup is comprehensively described in a series of publications (Kochkin et al. 2012; Kochkin et al. 2014, 2015; Nguyen 2012; Nguyen et al. 2008; van Deursen and Kochkin 2015). Images were provided by two ultra high-speed intensified CCD cameras, which allowed exposures down to 1.2 ns. A 1 MV voltage pulse with 1.2/50 μs rise/fall time was applied between two conical electrodes. The distance between the electrodes varied between 100 and 175 cm.

One may speculate that meter-long discharges are not sufficiently long to observe lightning features like space leader, and that meter-long discharges develop in the so-called final jump condition. But we will show that the first stages of a space leader development, the space stem and pilot system are present and can be studied in the laboratory. We also refer to one of the pioneering works by Les Renardieres (1981): "*The discharge phenomena in negative rod-plane gaps with separations greater than 4 m are also found in many cases to be remarkably similar to those observed for distances from 1 m down to 0.25 m.*" Thus, meter and microsecond sparks play an important role in understanding lightning and its related phenomena.

3.1. Inception

The discharge development always starts with an inception cloud of corona. As was shown in Clevis et al. (2013) voltage rise time significantly affects corona cloud formation and development. As a rule, such corona clouds appear at the highest electric field regions near the sharp edges of the high-voltage electrode. They continue to rise until the criteria for streamer propagation is fulfilled. Streamers appear from the cloud when the electric field on its edge exceeds a critical value. The critical electric field for positive and negative streamers is ~4.5 kV/cm (Allen and Ghaffar 1995) and ~12.5 kV/cm, respectively (Babaeva et al. 1997). The difference is due to the different directions of the flow of charged particles. Emergence of inception clouds and streamers in smaller gaps under different N_2-O_2 mixtures has been investigated by e.g., Chen and Heijmans (2015).

Figure 4 shows the very beginning of a negative meter-long spark development. The inception corona cloud and streamers coming from it, as well as streamers from the protection discs are clearly visible. The discharge electrical parameters and the camera shutter opening time are indicated on image (b).

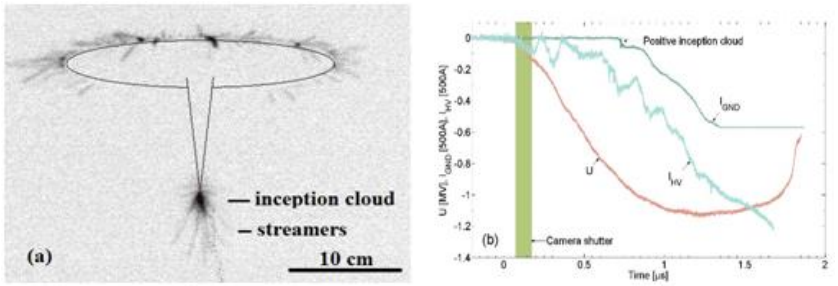

Figure 4. (a) The negative inception corona cloud at the HV electrode. The exposure time is 100 ns. (b) Electrical parameters of the discharge. The figure is reproduced from (Kochkin et al., 2014).

After about 0.7 μs of the discharge initiation, negative streamers from the HV electrode reach the grounded electrode and enhance the local electric field there. When the electric field is strong enough, a positive inception cloud ignites on the electrode tip. This process is depicted in Figure 5. The figure shows two consecutive images taken by two identical cameras with 20 ns exposure one after another. Original images are black and white and the applied color scheme is only intended to enhance visual perception, but does not represent the actual temperature of plasma processes. Clearly, after the inception cloud disappears, there are positive streamers moving upwards and a bright spot right at the electrode tip. The spot indicates that current still flows feeding the streamers. The current wave shapes are shown in Figure 4 panel (b).

A faint trace is visible in Figure 5 image (b) coming from the electrode tip to the right-top side. It is a camera artefact. The camera shutter is an electronic device, which is good but not perfect. Even when it is closed during the final breakdown, some light can leak through it and cause such traces. In other words, the trace shows where the final breakdown will go through. We consider it a feature and did not make any effort to reduce its appearance.

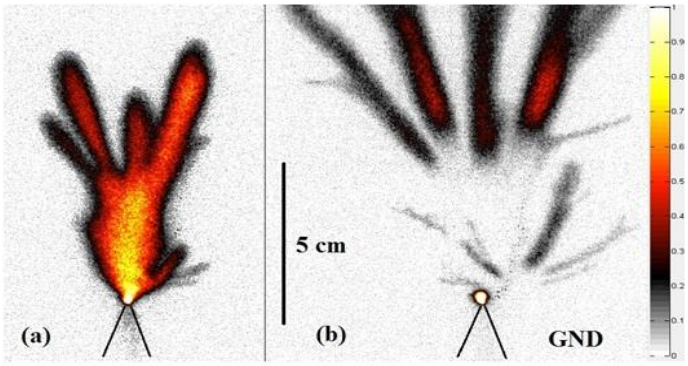

Figure 5. Two subsequent images of the positive inception cloud on the grounded electrode in negative high-voltage setup configuration. Each image has been made with 20 ns exposure time one after another. Figure reproduced from (Kochkin et al., 2014).

After the inception cloud breaks apart on different streamers, the streamer phase begins. Although individual positive and negative streamers appear similar on our images, the processes that drive them are different.

3.2. Streamer Propagation

Streamer propagation is highly dependent on parameters such as electric field, ambient conditions and gas mixture. In the used setup configuration, both negative and positive streamers propagate with similar speed $(2\pm1)\cdot10^6$ m/s slightly dependent relative to the electrode proximity. Stable propagation of streamers can be achieved on a high range of electric fields – from the critical minimum electric field mentioned above up to conventional breakdown field ~ 30 kV/cm in STP air (Qin and Pasko 2014). Streamers usually follow the electric field lines. However, as it was recently shown, streamer discharges can move perpendicularly to the electric field lines when an external source of ionization is introduced (Nijdam et al. 2014).

A very remarkable experiment is described in (Nijdam et al. 2013). There, it is shown that streamers can halt when the electric field is off and reignite if the field is shortly on again. Such streamer behavior might be closely related to appearance of bipolar structures in negative discharges, as will be shown below.

In (Kochkin et al. 2014) negative streamer branching angles were reported. It was shown that negative streamers split at 29±5º. Here we report that positive streamers branch at 35±7º adding that they experience less branching when they move in a forward direction (i.e., from HV electrode straight to the grounded) and more branching when they move laterally. This is due to a stronger electric field along the short path between electrodes. According to (Qin and Pasko 2014), when streamers move in more favorable conditions (i.e., stronger electric field) they keep their radius small preventing branching.

3.3. Leader Phase

Leader is a hot channel in contrast to streamers, which are cold plasma filaments. The main difference between leader and streamer is that the leader is always connected to the HV electrode independently on when the camera's shutter was opened and for how long. In shorter gaps of about 1 m, the hot channel appears when the streamers bridged the gap and established the first conductive channels between two electrodes. In longer gaps of 1.5 – 1.75 m the hot channel appears before bridging.

On both images of Figure 6, the leader channel is only 1 pixel thick. This means that the leader thickness is less than 0.5 mm and cannot be estimated with better precision with our camera and the attached optics. Ionization is visible at the leader tip that will eventually create a leader sheath of 3.5 cm thickness. Later, when positive and negative counter-leader meet the breakdown occurs.

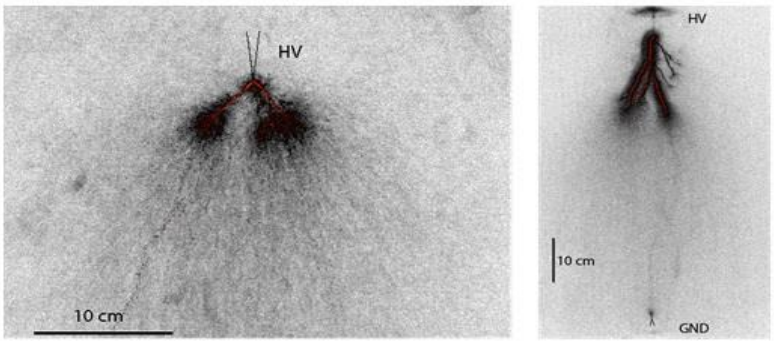

Figure 6. Left - positive leader in 144 cm gap, exposure time is 20 ns. Right – positive leader in 144 cm gap, exposure time is 50 ns. The leader propagation speed is $1.5 \cdot 10^6$ m/s.

3.4. Breakdown

The breakdown phase begins when two counter propagating leaders, positive and negative, meet at a certain point. In the discussed test, it happens at t = 1.7 μs in Figure 4 (b). At that moment, voltage drops, currents through both electrodes rise rapidly, heating up the channel(s) that lead to a bright arc. Photographing this moment with the high-speed camera is usually avoided due to the damage it may cause the image intensifier. However, this stage has recently been investigated and reported in Vayanganie et al. (2016), where it is shown that the laboratory leader decays similar to bead natural lightning.

4. Occurrence of X-Rays

The first laboratory observation of X-ray bursts from meter-long discharges in air was reported in 2005 by Dwyer et al. (2005). Later, many other different groups confirmed the finding also reporting similar measured physical parameters of such bursts (Dwyer et al. 2008; Kochkin et al. 2012, 2015; March and Montanyà, 2010, 2011; March 2011; Nguyen et al. 2008; Nguyen et al. 2010; Rahman et al. 2008; Rep'ev and Repin 2008). The observations by several groups coincided with the detection of at least one X-ray pulse before the breakdown of the gap.

After the first experiment by Dwyer et al. (2005), not many experiments to study and determine properties of X-rays generated from long laboratory sparks in air have been performed. There, in an experiment involving rod-plane geometry, 15 sparks of both polarities were applied, and X-ray detections were observed in 14 sparks and for both polarities. A 1.5 MV Marx generator was used and the gap distance ranged from 1.5 to 2 meters. This test started further X-ray laboratory research, as it was demonstrated that it was possible to observe X-rays from laboratory discharges.

Motivated by the results of Dwyer et al. (2005) test, Rahman et al. (2008) performed a test on 80 cm rod-hemisphere gap applying 83 negative lightning impulses (1.2/50 μs) using a 1

MV Marx generator. With this setup, for 49 out of 83 sparks (59% of the cases) X-rays were observed. X-rays were reported to occur around the peak current (47% of the occurrences), around the onset of the main discharge current peak, which coincides with the voltage collapse (45% of occurrences) or during both (8% of occurrences). From these results, it was concluded that the processes for X-ray emission were associated with streamer tips development and final jump processes for both types of emissions.

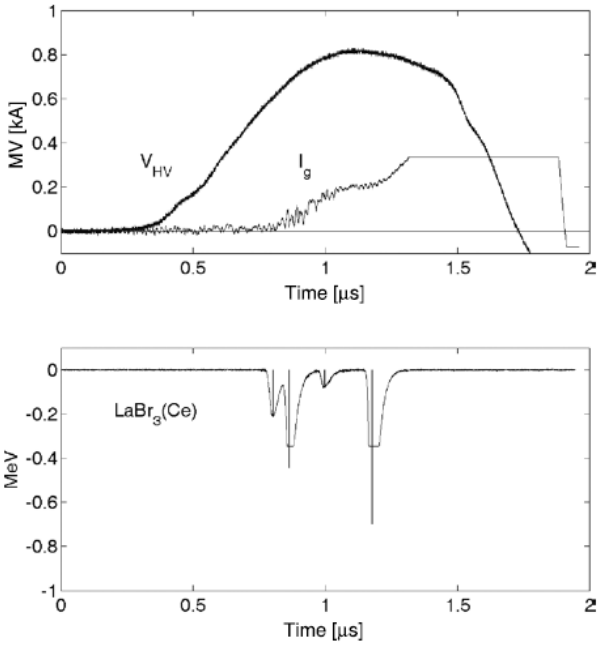

Figure 7. Positive surge with 810 kV peak, shown with the cathode current (Ig) during the leader initiation phase, with gap breakdown occurring at 1.5 μs (top). $LaBr_3$(Ce) detection of the high energetic particles extending from 0.8 to 1.2 μs (bottom). Vertical bars in the bottom figure indicate the maximum equivalent energy and its timing obtained by the fit. Reproduced from (Nguyen et al. 2008).

In 2008, two more tests were performed and published quasi simultaneously at the end of the year. In the first test by Nguyen et al. (2008), positive and negative polarity of standard lightning impulse voltage waveforms were applied to a rod-rod geometry with gap distances from 0.7 to 1.2 meters. All 50 positive polarity impulses resulted in hard energy emissions detected by a $LaBr_3$(Ce) detector. As the current from ground electrode was measured, for all cases, detections coincide with the increase in the current of the grounded electrode (cathode in that case). This can be observed in Figure 7. The majority of the detections occurred after about 75% of V peak. For negative polarity (20 sparks), much stronger signals were detected by scintillators as in the positive case, and occurrence of X-rays was similar as in the positive case. The work also presented a comparison of different scintillators NaI(Tl), LaBr(Ce) and

BaF_2 as well as an analysis of the energy reaching the detectors at different distances between the gap and the detector.

The second work in 2008 (Dwyer et al. 2008), presents a test comprising 231 sparks for both positive and negative polarities with gap lengths ranging from 10 to 140 cm. Five NaI(Tl) and one plastic scintillators are placed inside shielded cabinets. Different electrode configurations were used comprising sphere-sphere (from 2 to 12 cm in diameter), a rod-sphere or a rod-plane. They found that a much higher percentage of detections occurred for negative polarity (70%) than for positive polarity (10%). X-rays timing differ for positive and negative polarities; for negative polarity, X-rays were identified to occur at two distinct times of the discharge: near the peak voltage and coinciding with voltage collapse (breakdown time). For positive polarity, X-rays detections only occurred near the peak voltage. As the laboratory was the same as in Rahman et al. (2008), for which X-rays also occurred near the voltage collapse for negative polarity, they used collimators in order to determine the spatial source of both X-rays for negative polarity. The first X-rays resulted to originate from the gap while the second X-rays appeared to originate from above the gap in the space over the high voltage components. In Figure 8, X-ray detections are plotted as well as the voltage waveform for negative and positive polarity discharges as presented in Dwyer et al. (2008).

After those four laboratory experiments, no more tests were performed on long laboratory sparks in air until 2010. Tests in the 2005-2008 period were composed of a total of ~400 sparks. The design of these tests was more focused on detecting X-rays or determining occurrence for positive and negative polarities. From these four tests, the following properties may be identified:

- X-rays can be generated within the air gap in laboratory conditions with the use of fast voltage impulses (Dwyer et al. 2005).
- Negative impulse voltages lead to higher detection rates as well as higher energetic particles (Nguyen et al. 2008; Dwyer et al. 2008).
- X-rays for positive sparks occur near the peak of the applied voltage (Nguyen et al. 2008; Dwyer et al. 2008).
- X-rays for negative sparks occur at two distinct times: near the peak of the applied voltage (Rahman et al. 2008; Nguyen et al. 2008; Dwyer et al. 2008) and near the voltage breakdown (Rahman et al. 2008; Dwyer et al. 2008).
- Using collimators, it is found that X-rays detections near the peak voltage occurred within the gap, while X-ray detections near breakdown time occur above the gap (Dwyer et al. 2008).

During the period 2010-2014, five new experiments were performed by two different groups, with the aim of determining X-rays features for positive and negative polarities (Kochkin et al, 2012; Kochkin et al. 2014), the effect of the rise time (March and Montanyà 2010), the role of anode and cathode local electric fields (March and Montanyà 2011) and the influence of the gap distance (March et al. 2012). It is important to mention that data analysis from those tests is based on a total of more than 3800 sparks. Some of these tests are inspired from results and findings from tests during the 2005-2008 period. It is worth mentioning that thanks to the tests performed in the previous period, the design of the tests in this second period became possible. In this second period, Kochkin and colleagues (Kochkin et al. 2012; Kochkin

et al. 2014) focused on analyzing positive and negative discharges separately. They used a high-speed intensified CCD camera to capture discharge development of meter discharges. They found that for positive polarities, X-rays are time coincident with positive and negative streamers encounters. This occurred near the peak voltage of the applied impulse (Kochkin et al. 2012). For negative polarity, X-rays emissions occur before the onset of the ground current (anode), coinciding with initiation of high voltage electrode activity (cathode). X-rays are correlated to streamers advancement, promoted by encounters of positive and negative streamers of negative discharge development process (see section 3 of this chapter).

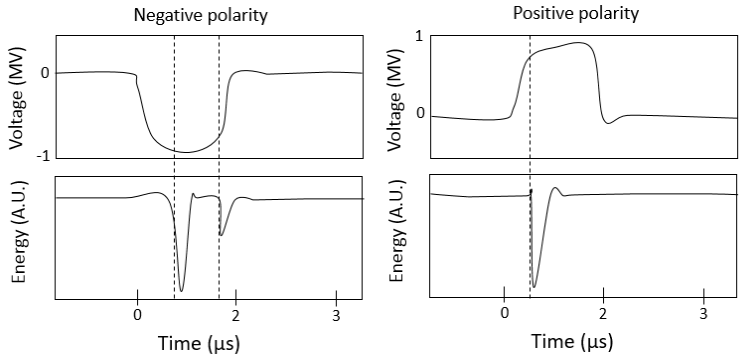

Figure 8. Sketch of negative (left) and positive (right) polarity tests showing X-ray detections and voltage waveforms. For negative polarity, the two X-rays pulses near the peak voltage and near breakdown can be identified while for positive polarity X-rays only occurred near the peak voltage. This sketch is based on Dwyer et al. (2008).

From this new set of tests, some conclusions can be extracted:

- X-rays from positive discharges occur at the onset of the cathode activity (Kochkin et al. 2012).
- X-rays are influenced by cathode geometry (March and Montayà 2011; Kochkin et al. 2012) while anode geometry does not influence X-ray emission.
- An increase of the peak voltage leads to an increase of detection percentage and average energies of X-rays emitted from the gap (March and Montanyà 2010; March and Montanyà 2011; March et al. 2012).
- Rise time of the applied impulse determines X-ray detection percentages for a given geometry (March and Montanyà 2011).
- Gap breakdown is not a necessary condition for X-ray emission (March et al. 2012; Kochkin et al. 2014).
- Occurrence of X-rays for positive polarity is linked to the encounter of positive and negative streamers (Kochkin et al. 2012) while for negative polarity it is linked to negative streamers development (Kochkin et al. 2014).

Although the most recent experiments showed that the X-ray emissions are related to streamer encounters, this was recently modelled by Ihaddadene and Celestin (2015) where it was shown that the electric field in a head-on collision could indeed reach values higher than required for the cold run-away breakdown. However, the electric field quickly collapses due to the increase of background ionization, leaving no time for the electrons to accumulate sufficient energy. Thus, it was concluded that a streamer encounter is unlikely to generate the detected X-ray bursts. Nevertheless, the boundary conditions with fixed potential used in the model lead to underestimation of the electric field.

Table 1 summarizes laboratory tests performed since 2005, in determining properties of X-rays from long sparks in air.

Table 1. Summary of laboratory tests on X-ray emissions from long sparks in air at atmospheric pressure

Reference	Experiment details	Test objective	Findings
Dwyer et al. (2005)	Rod-Plane 14 sparks Both polarities Gap distances 1.5-2 m Rise time 1.2 μs 3 x NaI(Tl)	Determine if X-rays can be observed in laboratory sparks	X-rays are observed for both positive and negative sparks X-rays coincided with triggering of Marx generator spheres, near peak voltage and before voltage collapse (only for negative)
Rahman et a. (2008)	Rod-Hemisphere 83 negative sparks Gap distance 80 cm Rise time 1.2 μs 1 x BaF_2	Confirm (or refute) the production of X-rays by long laboratory sparks	Production of X-rays in laboratory is confirmed X-rays generated near peak voltage and breakdown First X-rays associated with runaway electron in streamer tips and second with final jump
Nguyen et al. (2008)	Rod-Rod 50 positive and 20 negative sparks Gap distance 1.2 m Rise time 1.2 μs 1 x NaI(Tl) 1 x $LaBr_3$(Ce) 1 x BaF_2	where and when in the developing discharge channel the high-energy radiation is generated	Positive sparks: X-rays occur when cathode current starts to rise. Pile-up of X-rays are detected by scintillators Negative sparks: X-rays originate not only from the spark gap, but also formed elsewhere if the local electric field is large enough for discharge initiation.
Dwyer et al. (2008)	Multiple geometries (sphere-sphere, rod-sphere, rod-plane) 231 sparks Both polarities Gap distances from 10 to 140 cm Rise time 1.2 μs 5 x NaI(Tl) 1 x plastic	Investigate X-ray emission from long laboratory sparks in air	X-rays produced by both positive and negative sparks X-rays are produced in gap lengths of 20 cm X-rays often occur near peak voltage Second X-rays often occur when voltage across the gap is collapsing

Reference	Experiment details	Test objective	Findings
March and Montanyà (2010)	Rod-Rod and Rod-Plane 450 positive sparks Gap distance 58 cm Rise times 0.66, 1 and 2 μs 1 x NaI(Tl)	Determine influence of the voltage and rise time on the detection of X-rays during spark discharges at the laboratory. Study the influence of the positive and negative polarities on the X-rays emission.	Rod-Rod test (+ sparks): Increasing peak voltage both detection percentage and energies increase Average energy and detections' percentage show the influence of the voltage derivative parameter (dV/dt) Emissions occur around the peak voltage Rod-Plane test (+/- sparks): lack of detections with positive polarity suggests the influence of the discharge mechanism on the production of X-rays
March and Montanyà (2011)	Rod-Variable Rod (0, 12, 17 and 42 cm) 165 positive and 150 negative sparks Gap distance 58 cm Rise time 600 ns 1x NaI(Tl)	Show the influence of the positive and the negative electrodes in the production of runaway electrons in laboratory sparks	Emissions are influenced by the negative electric field distribution at the cathode.
Kochkin et al. (2012)	Rod-Rod 951 positive sparks Gap distance 1 m 2 x $LaBr_3$(Ce)	Investigate structure and evolution of long positive spark breakdown; and study at which stage pulses of X-rays are emitted	Presence of negative streamers is necessary condition for X-ray generation X-rays correlate in time with the encounter of positive and negative streamers Increasing the number of streamers with special cathode increased the occurrence of X-rays
March et al. (2012)	Rod-Rod 315 positive sparks Gap distances of 46, 58, 68 and 84 cm Rise time 600 ns 1 x NaI(Tl)	Analyze X-ray detection within gap only varying gap distance	Gap breakdown is not a necessary condition to detect X-rays. Saturation (in detection rate) can occur for small gap length.
Kochkin et al. (2014)	Rod-Rod 1800 negative sparks Gap distances of 107, 145 and 175 cm Rise time 1.2 μs 2 x $LaBr_3$(Ce)	Investigate the development of meter long negative discharges and focus on their x-ray emissions.	Nanosecond-fast x-ray bursts happen during the prebreakdown process; the final breakdown of the gap is not necessary. It is most likely that streamer encounters are responsible for the x-rays

Apart from the features and findings presented in those sections, in two tests (e.g., March et al. 2012; Kochkin et al. 2012) X-rays with no gap breakdown were detected. In the case of (March et al. 2012) it was detected for positive polarity spark (shown in Figure 9) and in case of (Kochkin et al. 2014) for negative polarity.

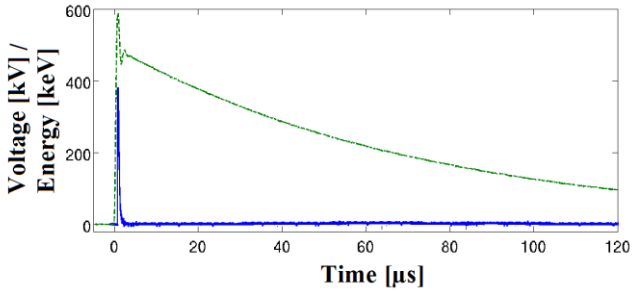

Figure 9. Positive impulse voltage and X-ray detection for rod-rod geometry. X-ray was detected near the peak voltage of the applied impulse, when no breakdown occurred across the gap during the experiments by March et al., (2012).

4.1. Features of X-Rays in Positive Discharges

Positive discharge development in time-integrated images was shown in (Kochkin et al. 2012) and reproduced here for consistency. The discharge starts with formation of a positive corona at the HV electrode tip and protective aluminium dish (see Figure 10). The dish and tip are indicated in image (a) by arrows. Clouds of positive streamers emerge from the HV electrode and propagate downwards with $2 \cdot 10^6$ m/s. The positive corona brings part of the potential to the grounded (GND) electrode and enhances the local electric field on its tip and sharp edges. If the enhanced field is strong enough (typically happens on relatively short gaps of 1 meter), the negative counter-streamers can emerge from the GND electrode. The positive streamers merge with the negative ones in head-on collisions and establish the first conductive channels between two electrodes. The Ohmic heating of these streamer channels leads to appearance of bright hot arc/leader (see images j – o). The streamer collisions are accompanied by high-frequency oscillations at the ground current probe. The amplitude of such oscillations positively correlates with the X-ray appearance. No X-rays have ever been detected before the current went through the grounded electrode.

The X-rays appear in ns-fast bursts, meaning that rather fast process is responsible for their generation. This observation challenges the idea that negative streamers themselves can produce such X-rays. More details on X-ray detection and their physical properties can be found in (Kochkin et al. 2012).

The electrical characteristics of the positive discharge are shown in Figure 10 at the bottom panel. Voltage rise begins at t = 0 s and breakdown happens at t = 1.5 µs. Gap distance is 1 meter. High-frequency oscillations on the ground current probe are visible at t = 0.7 and 0.8 µs. The X-ray burst is detected just before the second high frequency current oscillation. The first high-voltage current at t = 0.2 µs corresponds to inception cloud formation at the HV electrode tip. The HV current peak at t = 0.4 µs corresponds to the positive streamer emergence from the protective dish. The camera shutter always opens at t = 0.36 µs (z line) and closes at different times (a – o lines). Thus, each image is time-integrated over the shutter opening time. Every image represents single different discharge. The bottom plot shows electrical characteristics of image (l).

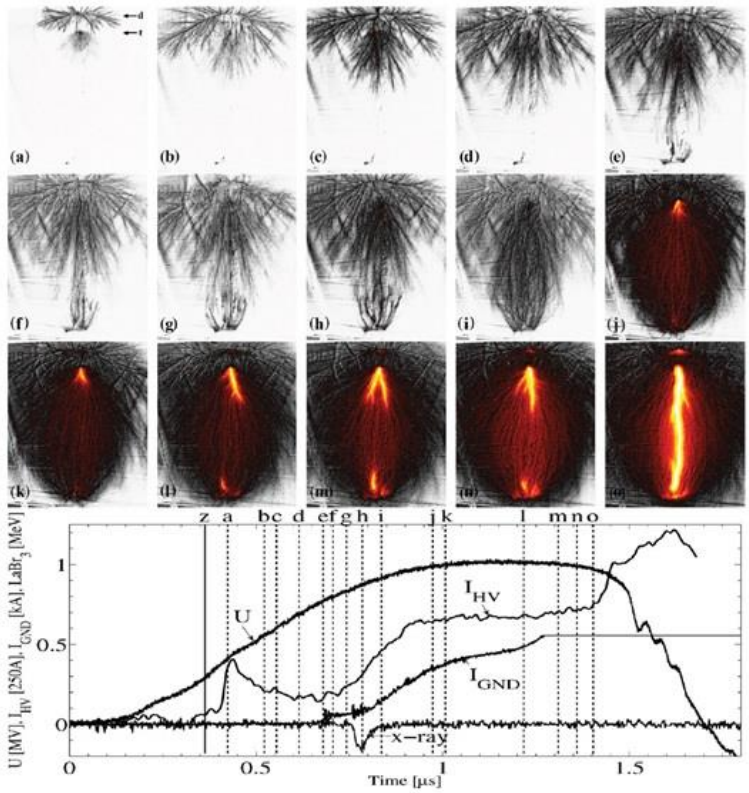

Figure 10. Positive discharge development in time-integrated sequences of 15 different discharges (images a-o). Gap distance is 1 meter. Exposure time varies between 60 ns (image a) and 1000 ns (image o). Shutter opening time is indicated by line Z on the bottom plot. Bottom panel shows electrical characteristics of the discharge (l). Reproduced from (Kochkin et al., 2012).

Figure 11 shows the grounded electrode at the most intense X-ray time. Positive streamers from the HV electrode merge with the negative counter-streamers. Such encounters enhance the electric field between two streamers lead to values higher than required for the cold run-away breakdown.

Figure 12 shows an alternative grounded electrode with 75 sharp spikes used to increase the number of counter-streamers and consequently streamer encounters. According to our expectations, this would lead to a significant increase in X-ray production.

Figure 13 demonstrates the alternative grounded electrode at work. Clearly, the number of negative counter-streamers increased. X-ray measurements have shown 10 times more bursts and associated high-frequency oscillations in this configuration.

As was shown in Ihaddadene and Celestin (2015), streamer encounters may leave glowing beads. On the left-hand side of Figure 13, glowing beads are clearly visible not only on the surface of the electrode, but also in the air.

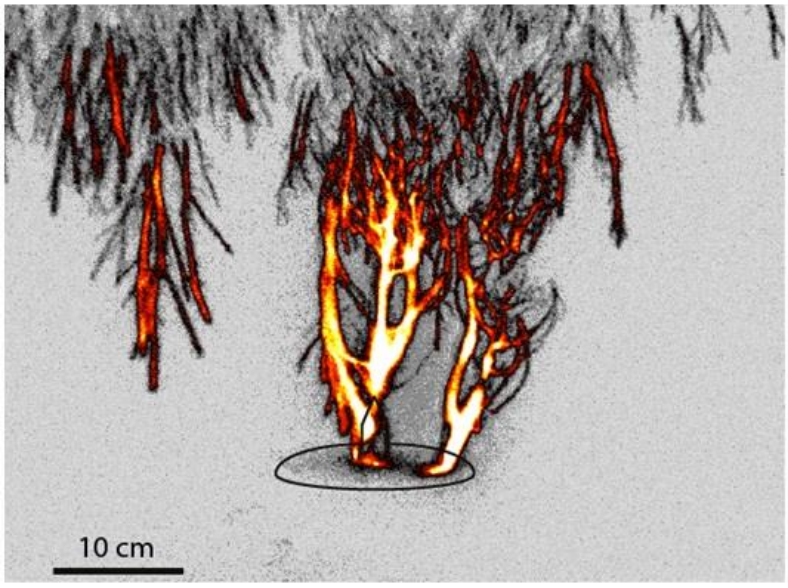

Figure 11. Zoom in on the grounded electrode at the most intense X-ray time. Positive streamers from the HV electrode encounter negative counter-streamers and the GND electrode. Exposure time is 50 ns.

Figure 12. Alternative grounded electrode with 75 spikes to increase the number of negative counter-streamers. Reproduced from (Kochkin et al., 2012).

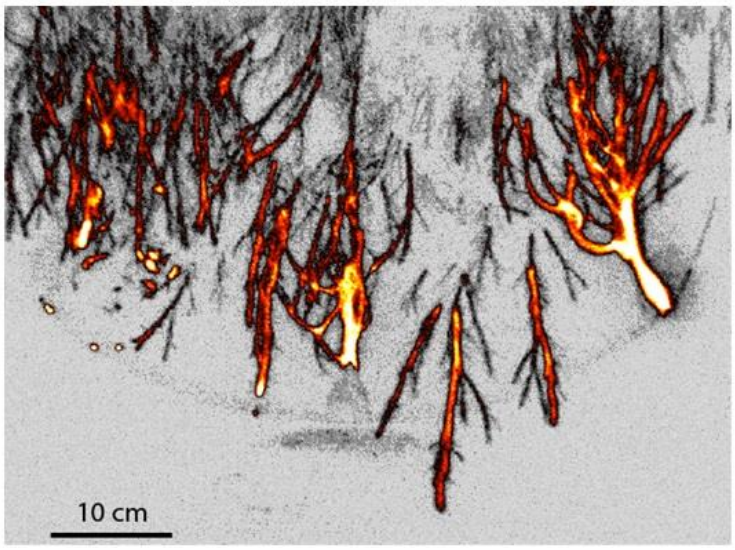

Figure 13. High-speed image (50 ns) of the alternative grounded electrode under positive HV pulse at the most intense X-ray time.

4.2. Features of X-Rays in Negative Discharges

Negative meter-scale discharge development was demonstrated in (Kochkin et al. 2014) and its X-ray emission in (Kochkin et al. 2015). Statistical analysis of the X-ray emission was published in (Carlson et al. 2015).

Due to higher electric field requirement for stable negative streamer propagation, negative discharges possess more complex development processes than positive. Negative discharges are known to develop via formation of bipolar structures in front of the leader tip. The existence of bipolar structures was first demonstrated in 1962 by Stekolnikov and Shkilev (1962). Such structures were never documented in positive discharges. A more comprehensive study of the negative discharge development process has been done by Les Renardieres group (Les Renardieres 1981). The precise mechanism of the bipolar structure formation was shown in (Kochkin et al. 2014) with ns-fast photography and reproduced here. Such bipolar formations are called “pilot systems” or pilots for short.

Figure 14 shows the pilot system development. The camera points just below the HV electrode. A negative streamer leaves isolated dots (beads) behind during its propagation (see image (a)). Sometimes the dots are branching points of the negative streamer. Later the dots launch positive streamers in the opposite direction (image (b) and (c)). The positive streamers move towards the HV electrode branching and merging with new negative streamers (image (c) and (d)). The bipolar structure – negative streamers, dots and positive streamers is called a “pilot system.” The pilot system appearance coincides in space and time with X-ray bursts. In longer gaps such systems may develop into space leader.

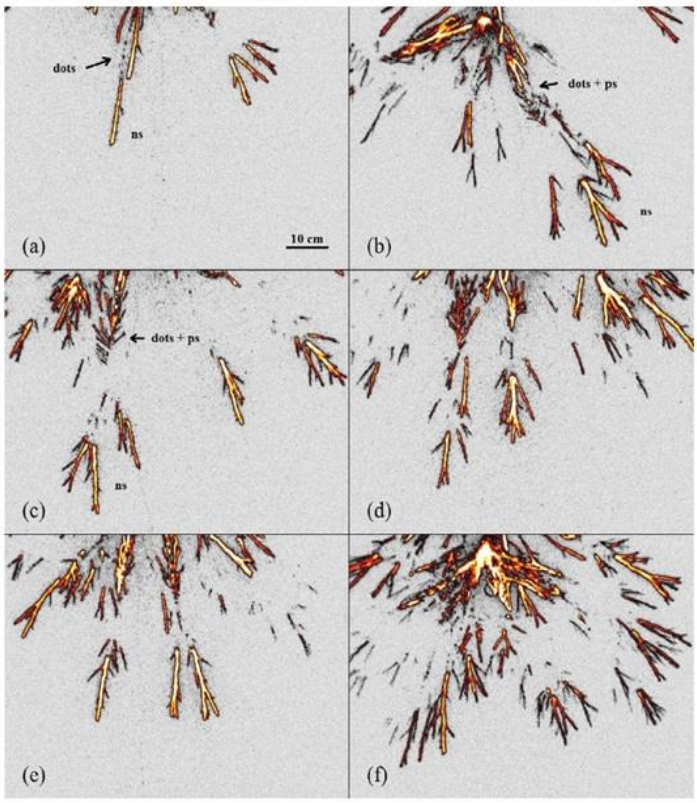

Figure 14. Pilot system development process. Negative streamers leave isolated beads behind. Positive streamers emerge from the bead and propagate towards the HV electrode. Reproduced from Kochkin et al. (2014).

The beads can be called a space stem for consistency with previous studies. However, we stress that they appear not in virgin air as was thought for the space stem but as result of negative streamer propagation. It was reported in (Les Renardieres 1981) that the space stem can move into the gap with the speed of $(2 – 20)\ 10^4$ m/s. This effect happens due to consecutive launching of positive streamers from the first bead to the next. Naturally, with streak photography techniques such propagation will appear as a moving space stem.

The last bead appears at the point where an instantaneous electric field equals the stability field for negative streamer. It means that the streamer experiences a shortage in electric field strength during its propagation and starts beading. The beads can be caused by brief halting of the streamer and consecutive reignition as described in this experiment (Nijdam et al. 2013). Since the stability field for the positive streamer is twice as small, positive discharge development is usually continuous and does not show beading or stepping behavior. Moreover,

the electric field behind the positive corona front is also smaller and might not be sufficient to create negative counter-propagating streamers.

4.3. Effect of the Peak Voltage and Voltage Rise Time

Runaway electron mechanism theory developed by Gurevich (Gurevich, 1961) as well as the mechanism for acceleration of electrons due to the high electric fields inside thunderclouds by Wilson (Wilson, 1925) share a main principle: high electric fields are required to accelerate electrons to relativistic energies. Translated to a laboratory environment, the appearance of X-rays from Bremsstrahlung of high energetic electrons should be related to peak voltage applied to an electrodes' gap. This simple experiment can help comprehension that applying higher voltage across the gap increases the electric field between the electrodes, and according to the basic principle given by Lorentz Law ($F=q\cdot E$), the energies as well the number of runaway electrons should increase. In other words, the efficiency of runaway electrons process in a specific gap shall increase with an increase of the applied voltage.

The relationship between applied peak voltage with detection rate and average energy has been analyzed in different works (March and Montanyà 2010; March and Montanyà 2011a; March 2011 b; March et al. 2012) for both positive and negative polarities.

The influence of the voltage rise time derivative was investigated in an experiment performed by (March and Montanyà 2010). This experiment was designed based on results from previous laboratory experiments (Dwyer et al. 2005; Rahman et al. 2008 and Nguyen et al. 2008, March et al. 2010). In those experiments, it was found that X-rays were detected close to the peak voltage of the applied impulse (Figure 15). This experiment was also motivated by field observations of X-rays, as those observations correlated the appearance of X-rays with stepped-leader phase during downward lightning approach to the earth (Moore et al. 2001, Montanyà et al. 2014), and the known relationship between voltage derivative and streamer and leader velocities from laboratory sparks (Bazelyan and Rayzer, 1998).

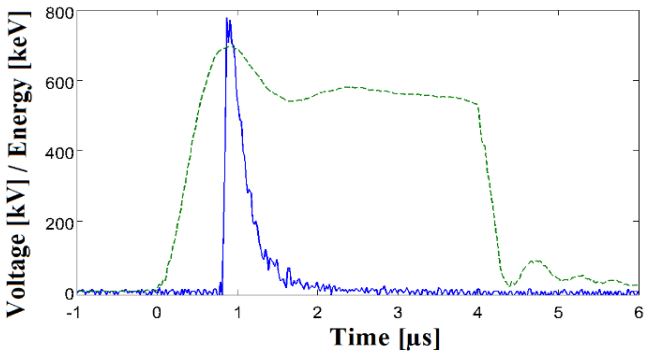

Figure 15. X-ray detection obtained by the authors. X-ray occurs near the peak voltage of the applied impulse.

The experiment consisted of 450 positive polarity sparks, 18 series of 25 sparks each. The setup consisted of rod-rod geometry spaced 58 cm and with a 3"x3" NaI (Tl) scintillator at 1.2 meters in perpendicular direction from the center of the gap. The Marx generator was adjusted to supply impulse voltages with three different rise times: 0.6, 1 and 2 μs. Generator adjustment details for rise time and peak voltage are described in section 2.1 of this Chapter.

In high voltage engineering (e.g., Kuffel et al. 2000), the term U50% is defined, which is a value of a 50% probability to breakdown. This value reduces with an increase of the applied rise time. So, for the 660 ns rise time the U50% value is higher than for the 1 and 2 μs rise times. On the contrary, it was found that the minimum voltage for X-ray detection occurred for the 660 ns rise time. In high voltage engineering, it implies that 660 ns rise time impulses required the lower overvoltage.

Table 2. $U_{50\%}$ breakdown voltage and minimum voltage for X-ray emission. Created with data from March and Montanyà (2010)

Rise time (μs)	$U_{50\%}$ Breakdown Voltage (kV)	Minimum Voltage for x-ray detection (kV)
0,66	425	430
1	380	440
2	346	480

The applied series of impulse voltages with different rise times showed that increasing the peak voltage for the same rise time leads to an increase of both detection percentage as well as average energy of detected X-rays. Focusing on the variation of the rise time, the faster the rise time the higher the detections' percentage and average energies than for slower rise times. Results for both detection percentage and average energies are plotted in Figures 16 and 17. From the results of this test, it can be concluded that faster rise times as well as higher peak voltages applied to the gap may enhance X-ray detection probability as well as average energies of detected X-rays.

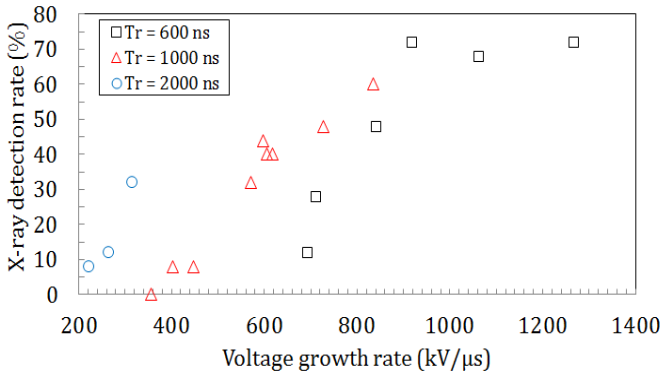

Figure 16. Detection percentage as a function of the voltage derivative for three different rise times. Created from data presented in March and Montanyà (2010).

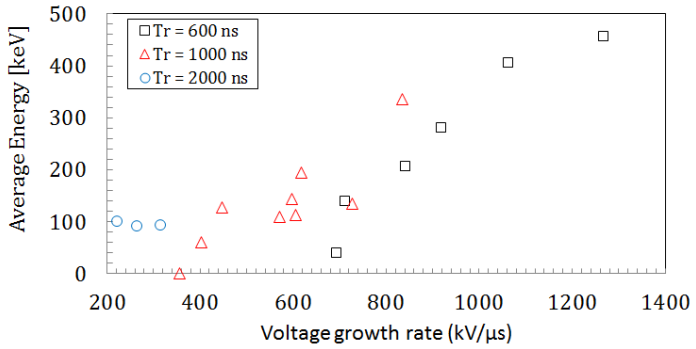

Figure 17. Average energy as a function of the voltage derivative for three different rise times. Created from data presented in March and Montanyà (2010).

4.4. Effect of the Gap Configuration

Test setup (i.e., anode and cathode shape and length, gap distance, waveform) may always be strictly defined in this kind of experiment, as these have a high influence in the results. Electrodes' geometries as well as distance between electrodes (gap distance) influence the local electric field close to the electrodes and the average electric field within the gap. Up to now, three experiments have been performed in this way for long sparks in laboratory conditions. March and Montanyà (2011) and Kochkin et al. (2012) executed two tests in which the shape of the cathode or the anode were varied in order to analyze the enhancement of the local electric field the electrodes may promote. In the case of March and Montanyà (2011), this was done by means of varying the length of one of the electrodes and applying both polarities to a fixed length electrode; while in Kochkin et al. (2012) the cathode shape was modified in positive rod-rod geometry. Another experiment was conducted using a rod-rod but varying the gap distance (March et al. 2012). In this experiment, the local electric field across the gap can be maintained constant using a spatial correction based on the relationship between voltage and electric field. These two modifications are described in the next sections.

4.4.1. Variation of Electrode Shape in One of the Electrodes

In March and Montanyà (2011) an experiment was performed using a constant rod to the energized electrode while for the grounded electrode the length of the rod was varied to 0, 12, 17 and 42 cm. In order to study the effect of positive and negative polarities close to the grounded electrode, both polarities were applied. Eleven series of the 15 sparks were performed for positive and negative polarity, resulting in a total of 165 for positive and 150 for negative polarity. As in previous experiments, it is very useful to obtain the U50% breakdown voltages of the different setup geometries to determine the test conditions from a high voltage engineering perspective. The resulting breakdown voltages are shown in Table 3. From results, it can be seen that for both positive and negative polarities and the particular configuration, U50% breakdown voltages are the same for all three rod-rod geometries (around 420 kV for positive and 475 kV for negative). Negative U50% breakdown voltage is also higher as for

positive, as usual in long laboratory sparks. For rod-plane geometry (this is when length of the earthed electrode is 0 cm), breakdown voltages differ from those values, especially for negative polarity. From the results of the U50%, it can be concluded that for rod-rod geometry this local variation of the electric field of the grounded electrode does not introduce any modification to the breakdown process more than the purpose of the test.

Table 3. U50% Breakdown Voltage for Positive and Negative polarities for the four different ground electrode configurations. Created from data presented in March and Montanyà (2011)

Earthed electrode length (cm)	Positive $U_{50\%}$ Breakdown Voltage (kV)	Negative $U_{50\%}$ Breakdown Voltage (kV)
0	389	590
12	412	475
17	425	475
42	420	470

Complete results can be found in the paper by March and Montanyà (2011). Here, only the rod-rod geometry results were analyzed. As the objective was to determine the possible influence the local electric field may have in the runaway electron process, detections percentage for positive and negative polarity are plotted in Figures 18 and 19.

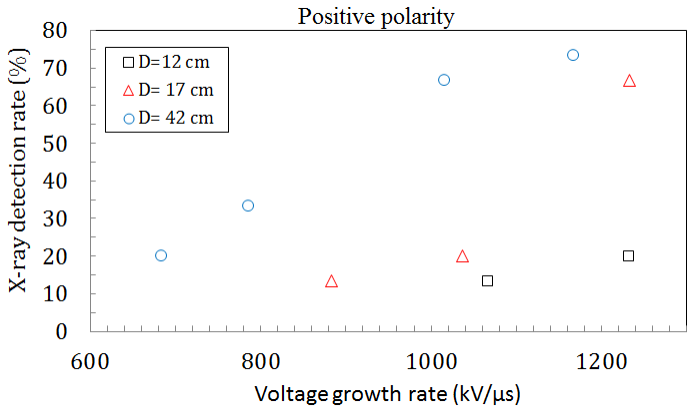

Figure 18. X-ray detection percentage as a function of the voltage-time derivative for rod-rod geometry with positive polarity and for cathode lengths of 12, 17 and 42 cm. Created from data presented in March and Montanyà (2011).

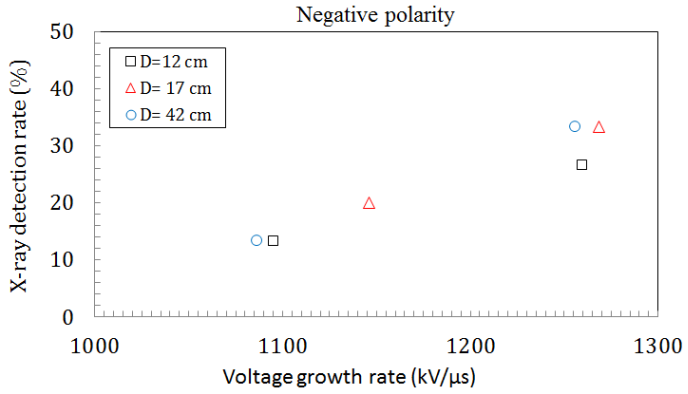

Figure 19. X-ray detection percentage as a function of the voltage-time derivative for rod-rod geometry with negative polarity and for anode lengths of 12, 17 and 42 cm. Created from data presented in March and Montanyà (2011).

Results from positive polarity in Figure 18 show that there is an increase of detection percentage rate with an increase of the length of the electrode. For example, at a voltage derivative of around 1000 kV/µs, the percentage of detections are around 10%, 20% and 70% for the 12, 17 and 42 cm earthed rod length, respectively. In other words, the required voltage derivative or peak voltage to obtain X-rays from the gap is lower for a longer earthed cathode. However, reader should note the highest point for the 42 cm anode rod length. According to linearity for the other 3 points, a detection percentage of around 100% would be expected. This result is discussed in the next section with information derived from another test.

For negative polarity (i.e., for varying anode's length), it can be seen that the points describe a lineal trend with respect to voltage derivative increase. Percentage of detections is almost the same for the different anode lengths and voltage derivatives. So, from this test it can be concluded that for rod-rod geometry, there is an influence of the cathode shape in percentage of emissions while the anode is not playing any role.

Same influence of the cathode shape was found in Kochkin et al. (2012). As presented in section X4.1, the use of an alternative grounded cathode composed of 75 spikes (Figure 12) to increase the number of streamers incepted from the cathode, resulted in an increase in the number of X-rays detected from the discharge. For the test conditions in Kochkin et al. (2012), modification of cathode geometry resulted in an increase of X-ray occurrence from 7% without the modified cathode up to 70% with the modified cathode.

4.4.2. Variation of Gap Distance

Spatial distance as well as the applied voltage between two electrodes determines the distribution of the electric field across the gap. According to runaway electrons theory (Gurevich 1961) and the electron acceleration mechanism established by Wilson (1925), electric field distribution may influence the acceleration process. In the previous section regarding the influence of the applied peak voltage, the rise time of the applied impulse voltage and the effect of the electrodes' geometry have been described. From a high voltage engineering

point of view, the other parameter to be analyzed is the gap distance, to determine whether it has any influence on the runaway electron process within the gap. The work by March et al. 2012 was focused on the investigation of the effect of the gap length. The experiment was performed using the same rod-rod geometry as in previous section (with a fixed cathode length of 42 cm), and with four different gap distances: 46, 58, 69 and 84 cm. The motivation for this experiment was the well-known fact in high voltage engineering that the electric field close to the electrodes is highly influenced by the electrode (Bazelyan and Raizer 1998). It means that for different gap distances, it is possible to have a very similar electric field close to electrodes by applying different voltages to the given distances that lead to the same electric field, as the electric field varies with the ratio of the applied voltage with distance. The rod-rod geometry used in this test promoted three different electric field regions within the gap. These three regions comprised two high electric field regions near the electrodes and a constant electric field region within most of the gap distance.

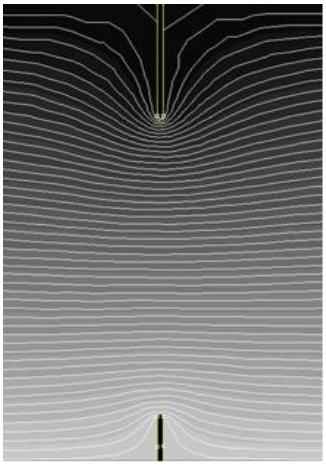

Figure 20. FEM simulation of the equipotential within the gap for the rod-rod geometry of the test. Electric field near the electrodes is enhanced and is a function of the geometry of the electrodes.

The presented test setup permitted the analysis of the influence of the gap distance in the production of X-rays. For each gap distance the relationship between the peak voltage and the percentage of X-ray detections was verified. Results clearly showed that in this experiment there is not only a relationship with peak voltage, but also with the gap distance. In this test, as smaller gap distances lead to higher electric fields within the gap for the same applied voltage to the electrodes, the percentage of detections is higher for the same peak voltage. This can be interpreted from Figure 21.

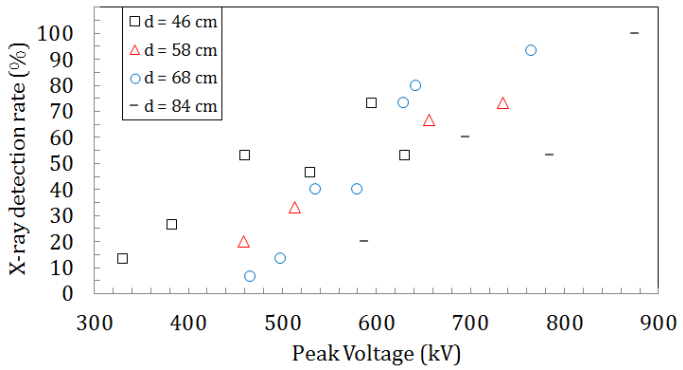

Figure 21. Detection percentage as a function of the peak voltage for different gap distances with same electrodes' geometry. Created from data presented in March et al., (2012).

The fact that shorter gaps produce higher number of X-rays detections rate, it could be possible that the correlation of the percentage of detected X-rays emissions would be higher when plotted as a function of the electric field. This is plotted in Figure 22 where the average electric field corresponds to V/d.

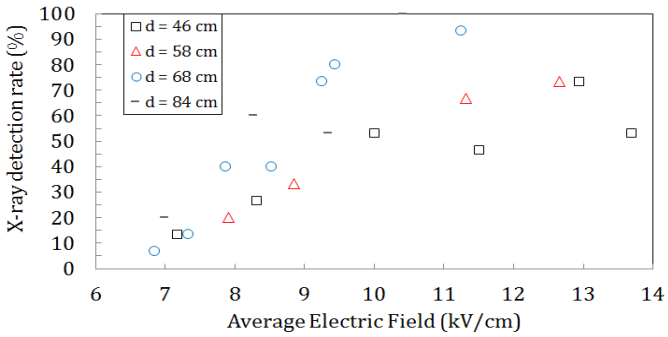

Figure 22. Detection percentage as a function of the average electric field (V/d) for different gap distances with same electrodes' geometry. Created from data presented in March et al. (2012).

In Figure 22, it can be seen that X-ray emissions for 68 and 84 cm gap length increase almost linearly with average electric field. Contrarily, the higher average electric field derivative values for the two shorter gaps diverge from the 84 cm trend line. Saturation can be observed for both shorter gap distances (46 and 58 cm gap length), and for this reason its dependence is not linear. At this moment, it is not possible to explain the reason for this gap saturation for shorter distances. However, it is interesting to determine correlations and dependency of the results. For this purpose, Pearson Correlation Coefficients (PCC) are presented as a function of different values and for all the points or removing saturation points for small gap distances.

One possible explanation for gap saturation might be related with streamer velocities. Streamer velocities increase for applied voltage derivative (Bazelyan and Raizer 1998). However, this increase is not linear, and it experiences a reduction in growth above a given value. As described in the above sections, a clear relationship between cathode activity and X-ray emissions was found in different tests. Therefore, it is possible that X-ray emissions saturate in the same way as negative streamer velocities slow their growth as a function of the voltage derivative. It is worth mentioning that results from Table 4 clearly show a significant increase of PCC for cases 2 and 3 when saturation points are removed. These results suggest a possible relationship between the average electric field or its derivative and detection percentages. Moreover, with high overvoltages applied to the gap, saturation of the process may occur. As said before, one possible explanation of X-ray emission within the gap might be related to negative streamer velocities, which are linked to voltage derivative.

Table 4. Pearson correlation coefficient for detection percentage points from test in March et al. (2012)

Points description	Pearson Correlation coefficient
Case 1 - All points as a function of peak voltage	0.644
Case 2 - All points as a function of average electric field	0.470
Case 3 - All points as a function of average electric field derivative	0.343
Case 1 except saturation points*	0.706
Case 2 except saturation points*	0.838
Case 3 except saturation points*	0.865

*We refer to saturation points the two higher points from the 58 cm gap and the 4 higher points from the 46 cm gap according to Figure 22.

4.5. Polarity Asymmetry

Polarity asymmetry in high voltage engineering is widely known for discharges in different media (liquid, solid or gas). In gases such as air, the process of streamer development for positive and negative streamers and required electric fields for streamer inception from an electrode are completely different. For example, negative streamers require an electric field two times higher than positives need for streamer propagation and the velocity of positive streamers are twice the velocity of negative streamers. Williams (2006) and Montanyà et al. (2015) described a similar problem of polarity asymmetry in lightning physics.

In the laboratory experiments presented in this chapter, polarity asymmetry is also present and attention must focus on distinguishing properties of the runaway electron process taking place in both polarities. As presented in previous sections (Kochkin et al. 2012) analyzed positive and negative streamer development in positive sparks using two intensified CCD cameras. From their results and observations of X-rays and positive and negative streamers developments, X-rays appear at the onset of the ground current (cathode), coinciding with the encounter of the positive and negative streamers. This is because when applying positive polarity to a rod electrode, negative streamers start to develop when positive streamers are almost reaching the ground electrode. Kochkin et al. (2012) found that “first X-ray photons

were detected immediately after the first cathode current oscillation." X-rays when accurately measured together with cathode current and image frames coincide with positive and negative streamers encounter. It is probably difficult for positive polarity discharges to promote setups in which the encounter of negative and positive streamers do not coincide in time with the start of cathode activity, due to high electric fields needed to feed the growth of negative streamers from the cathode grounded electrode.

For negative polarity, (Kochkin et al. 2014) found that X-ray emissions occur only with the onset of cathode activity, without onset of positive streamers from the grounded electrode. In this way, for negative polarity, the X-ray emission process depends only on negative streamers development, without the need for positive streamer activity from the opposite electrode. This finding undoubtedly links the runaway process with isolated advancement of negative streamer fronts.

Another interesting experiment with extreme asymmetry setup was performed by March and Montanyà (2010), with rod-plane geometry for both polarities. No detections were found for different peak voltages applied to a positive rod, while X-rays were detected in all the series for negative polarity. It is common in high voltage engineering that for positive rod-plane geometry negative streamers could not be incepted and only positive streamers could break down the gap, as the required electric field for negative streamer inception is not reached at plane cathode geometry.

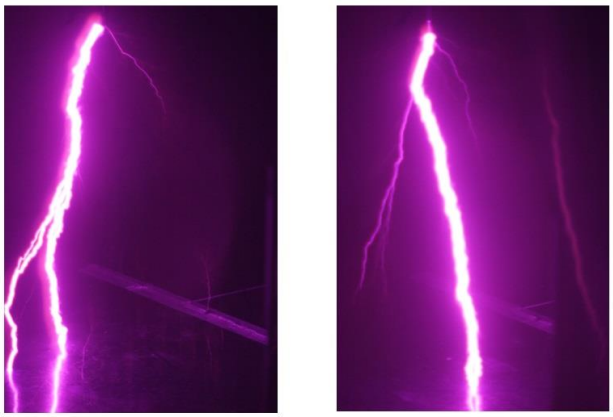

Figure 23. Negative rod-plane test with two visible positive streamers from the positive plane (left) and positive rod-plane test with multiple long positive streamers developing along the gap and without negative streamers from the negative ground plane (right). Images from test described in March and Montanyà (2010).

Another example can be found in (March and Montanyà 2011) where the shape of the ground electrode is varied for both polarities. X-ray emissions are highly affected by the shape of the grounded electrode for positive polarity and not for negative polarity. This also reflects the polarity asymmetry observed in production of X-rays from long laboratory sparks in air.

In (Dwyer et al. 2005; Dwyer et al. 2008; Nguyen et al. 2008) occurrence of X-rays is also affected by spark polarity, and in some cases this is affecting the timing of X-rays.

As conclusion, polarity applied to the gap on any test should be considered a discharge mechanism and may involve different physics affecting the occurrence of x-rays originated within the gap.

4.6. Measurements of Microwave RF Radiation and X-Rays

In lightning, the responsible X-ray emissions measured at ground is attributed to negative leaders, stepped leaders in virgin air and dart negative leaders. In the previous sections we described laboratory experiments that tried to reproduce these high-energy emissions. On the other hand, in lightning, negative leaders are also responsible for radio frequency (RF) radiation at frequencies from VHF to microwaves (Takagi and Takeuti 1963, Brook and Kitagawa 1964, Kosarev et al. 1970, Rust et al., 1979, Petersen and Beasley, 2013). These attributions to negative leaders raised the interest of Montanyà et al. (2015) who investigated RF emissions and X-rays on long laboratory sparks. In this work, the authors used a receiver tuned at 2.4 GHz with 5.5 MHz of bandwidth (Figure 24). The receiver includes a log-amp, which provides an output corresponding to the RF power within the band-pass frequencies.

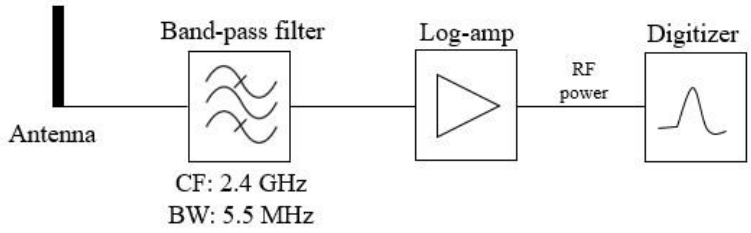

Figure 24. Schematic diagram illustrating the tuned microwave receiver used in Montanyà et al. (2015).

The results were that all of the applied impulses with and without breakdown produced microwave radiation for both negative and positive polarities. That was expected because of the popular use in high voltage RF detection of partial discharges. Nevertheless, the discovery was that in the cases with X-ray emissions, these emissions coincide with the peak RF power (Figure 25). This coincidence is resolved at the microsecond range since the detectors and the delays of the electronics used in the experiments do not allow better time discrimination. Moreover, the cases with X-rays detected the peak of the RF power tended to be significantly higher than the cases without detections.

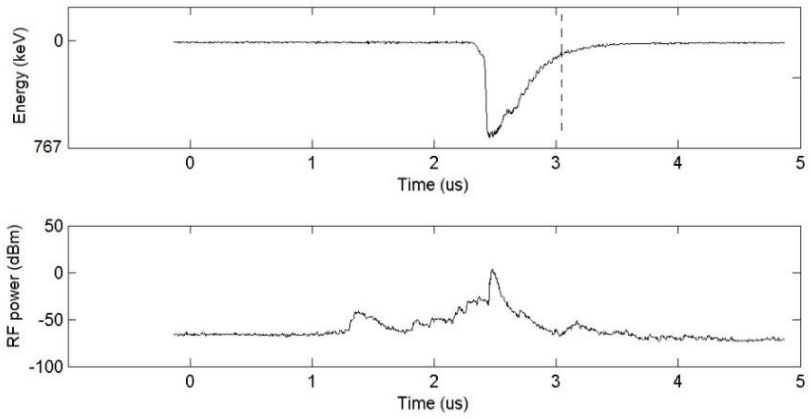

Figure 25. Example of simultaneous recording of and X-ray pulse provided by a NaI(Tl) detector and the described microwave receiver. Dashed line corresponds to the time of the breakdown of the gap.

The observations raise the question of why X-rays and the peak of RF occur so close in time. The coincidence can be due to similar mechanisms. The measured radiation can be related to the acceleration of electrons in streamers. However, this is not the only mechanism of production of X-rays. Bekefi and Brown (1961) studied bremsstrahlung radiation produced by accelerating electrons. When an electron makes a transition between two continuous states with initial and final energies of $\mathrm{mv}_\mathrm{i}^2/2$ and $\mathrm{mv}_\mathrm{f}^2/2$ respectively, it radiates and emits a quantum of $\hbar\omega$. This radiation forms a continuum. Rai et al. (1972), based on Bekefi and Brown (1961), found that the bremsstrahlung process is the possible source of UHF and microwave emissions related to lightning leaders.

To investigate the radiation of the accelerating electrons in streamers, a 1.5D model (1-4) as described in Bazelyan and Raizer (1998) is computed.

$$\frac{\partial n_e}{\partial t} = -\nabla \cdot \overrightarrow{v_e} + D_e \nabla^2 n_e + (v_i - v_a) n_e - \beta_{ep} n_e n_p + S_{ph} \quad (1)$$

$$\frac{\partial n_p}{\partial t} = v_i n_e - \beta_{ep} n_e n_p - \beta_{np} n_n n_p + S_{ph} \quad (2)$$

$$\frac{\partial n_n}{\partial t} = v_a n_e - \beta_{np} n_n n_p \quad (3)$$

$$\nabla^2 \phi = -\frac{e}{\varepsilon_o}\left(n_p - n_e - n_n\right) \quad (4)$$

where n_e, n_p and n_n are the electron, positive ion and negative ion densities, respectively. The electron drift velocity is $\overrightarrow{v_e} = -\mu_e \vec{E}$, where $\overrightarrow{v_e}$ is the electron mobility. D_e and v_i are the electron diffusion and the ionization coefficient, respectively. The attachment coefficient v_a is the addition of the two-body and three-body individual coefficients. Recombination coefficients are β_{ep} and β_{np} , which represent the electron-positive ion recombination and negative-positive ion recombination, respectively. The rate of electron-ion pair production due

to photoionization is S_{ph}. In Poisson's equation for the electric potential ϕ, e is the absolute value of the charge of the electron and ε_o is the permittivity of free space. The model represents the development of a mid-gap streamer. Figure 26 shows the electron density at different times during the first 6 ns.

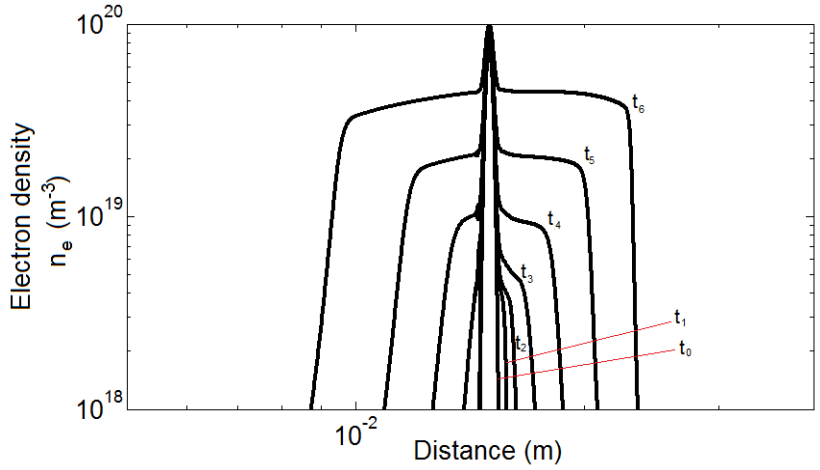

Figure 26. Electron density at different times (t_0= 0 s to t_6=6 ns) of a mid-gap streamer. Anode is to the left side and the applied field is E_o=2.7×10^6 V/m (E_k).

Once the electron density in time is determined, the flux of electrons is computed and the electromagnetic fields can be calculated. The radiation electric field component for the case of E_o=E_k and the case of E_o=5E_k are depicted in Figure 27. The cases of E_o=5E_k represent the 'overvoltage' situation typical in X-ray emissions in nanosecond voltage impulses and during the steps of lightning leaders. From the graph in Figure 27, a decrease of 20 dB at ~3.8 GHz can be shown, which for the cases of E_o=5E_k would be ~35 GHz.

The resulted spectrums demonstrate the radiated RF power, measured by Montanyà et al. (2015) at 2.4 GHz, can be due to the radiation of the accelerating electrons in the streamers during the streamer development in the gap. The calculations showed a cut-off of the spectrum in the computed streamer as a function of the applied electric field. In nature, high electric fields over E_k cannot persist for a long time. The case of 5E_k might even be so high to be found in long sparks and in lightning leaders. Further investigations are needed in order to determine the origin of the microwave radiation. Especially at frequencies of few tends of gigahertz where radiation produced by only the flux of electrons in streamers would collapse.

Comentado [JK1]: ? tens?

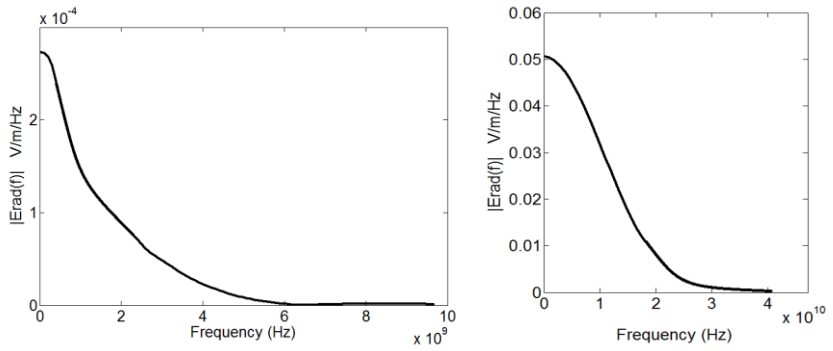

a b

Figure 27. Spectrum of radiation for the accelerating electrons in the computed streamer model. a) Case of $E_o=E_k$, and b) $E_o=5E_k$. The spectrums have been smoothed.

REFERENCES

Allen, N. L., and A. Ghaffar. 1995. "The conditions required for the propagation of a cathode-directed positive streamer in air." *Journal of Physics D: Applied Physics* 28(2): 331–37. Accessed March 16, 2016. doi:10.1088/0022-3727/28/2/016.

Babaeva, Nataliya Y., George. V. Naidis, 1997. "Dynamics of Positive and Negative Streamers in Air in Weak Uniform Electric Fields." *IEEE Transactions on Plasma Science* 25(2): 375–79.

Babich Leonid P., and Tat'yana V. Loiko. 2010. "Peculiarities of detecting pulses of runaway electrons and X-rays generated by high-voltage nanosecond discharges in open atmosphere." *Plasma Physics Reports*, 36(3):263–70.

Bazelyan, Eduard M., and Yuri P. Raizer. 1998. *Spark Discharge*. Boca Raton, New York, CRC Press.

Bekefi, George, and Sanborn C. Brown. 1961. "Emission of radio-frequency waves from plasmas." *J. Appl. Phys.* 32:25.

Brook, Marx, and N. Kitagawa. 1964."Radiation from lightning discharges in the frequency range 400 to 1000 Mc/s." *J. Geophys. Res.* 69(12):2431–34. Accessed March 16, 2016. doi:10.1029/JZ069i012p02431.

Carlson, Brant E., Nikolai Østgaard, Pavlo Kochkin, Ø. Grondahl, R. Nisi, K. Weber, Z. Scherrer, and K. LeCaptain. 2015. "Meter-scale spark X-ray spectrum statistics." Journal of *Geophysical Research: Atmospheres* 120(21):11191–202. Accessed March 16, 2016. doi:10.1002/2015JD 023849.

Chen, She, and Luuk C. J. Heijmans, Rong Zeng, Sander Nijdam, and Ute Ebert. 2015. "Nanosecond repetitively pulsed discharges in N2–O2 mixtures: inception cloud and streamer emergence." *Journal of Physics D: Applied Physics* 48(17): 175201. Accessed March 16, 2016. doi: 10.1088/0022-3727/48/17/175201.

Clevis, T. T. J., Sander Nijdam, and Ute Ebert. 2013. “Inception and propagation of positive streamers in high-purity nitrogen: effects of the voltage rise rate.” *Journal of Physics D: Applied Physics* 46(4): 45202. Accessed March 16, 2016. doi:10.1088/0022-3727/46/4/045202.

Cooray, Vernon, Liliana Arevalo, Mahbubur Rahman, Joseph R. Dwyer, and Hamid K. Rassoul. 2009. “On the possible origin of X-rays in long laboratory sparks.” *Journal of Atmospheric and Solar-Terrestrial Physics* 71(17-18): 1890–98. Accessed March 16, 2016. doi:10.1016/j.jastp. 2009.07.010.

Dorenbos, Pieter, Johan de Haas, and C.W.E. Van Eijk. 2004. “Gamma-Ray Spectroscopy with a 19 x 19 mm3 LaBr3:0.5% Ce3+ Scintillator.*” IEEE Transactions on Nuclear Science* 51(3):1289-96.

Dwyer, Joseph R., Hamid K. Rassoul, and Ziad Saleh. 2005. “X-ray bursts produced by laboratory sparks in air.” *Geophysical Research Letters* 32(L20809). Accessed March 16, 2016. doi: 10.1029/2005GL024027.

Dwyer, Joseph R., Ziad Saleh, Hamid K. Rassoul, Diego Concha, Mahbubur Rahman, Vernon Cooray, Jason Jerauld, Martin A. Uman and Vladimir A. Rakov. 2008. “A study of X-ray emission from laboratory sparks in air at atmospheric pressure.” *Journal of Geophysical Research* 113(D23): D23207. Accessed March 16, 2016. doi:10.1029/2008JD 010315.

Fishman, Gerald J., P.N. Bhat, R. Mallozzi, J.M. Horack, T. Koshut, C. Kouveliotou, G.N. Pendleton, C.A. Meegan, R.B. Wilson, W.S. Paciesas, S.J. Goodman, and H.J. Christian. 1994. “Discovery of intense gamma-ray flashes of atmospheric origin.” *Science* 264:1313–16.

Gurevich, Alex. 1961. “On the theory of runaway electrons.” *Sov. Phys. JETP* 12(5):904-12.

Ihaddadene, Mohand A., and Sebastien Celestin .2015. “Increase of the electric field in head-on collisions between negative and positive streamers.” *Geophysical Research Letters* 42(13): 5644–51. Accessed March 16, 2016. doi:10.1002/2015GL064623.

Kochkin, Pavlo O., Alexander P. J. van Deursen, and Ute Ebert. 2014. “Experimental study of the spatio-temporal development of metre-scale negative discharge in air.” *Journal of Physics D: Applied Physics* 47(14): 145203. Accessed March 16, 2016. doi:10.1088/0022-3727/47/14/145203.

Kochkin, Pavlo O., Alexander P. J. van Deursen, and Ute Ebert. 2015. “Experimental study on hard X-rays emitted from metre-scale negative discharges in air.” *Journal of Physics D: Applied Physics* 48(2):0225205. Accessed March 16, 2016. doi:10.1088/0022-3727/48/2/025205.

Kochkin, Pavlo O., Cung Vuong Nguyen, Alexander P. J. van Deursen, and Ute Ebert. 2012. “Experimental study of hard x-rays emitted from metre-scale positive discharges in air.” *Journal of Physics D: Applied Physics* 45(42):425202. Accessed March 16, 2016. doi:10.1088/0022-3727/45/ 42/425202.

Kochkin, Pavlo. 2014. “Understanding lightning: experiments on meter long discharges and their x-rays.” PhD diss., Eindhoven University of Technology.

Kosarev, E. L., V. G. Zatsepin, and A. V. Mitrofanov. 1970. “Ultrahigh frequency radiation from lightnings.” *J. Geophys. Res.* 75(36):7524–30. Accessed March 16, 2016. doi:10.1029/JC075i036p07524.

Kuffel, Edmunf, Walter S. Zaengl, John Kuffel. 2000. *High Voltage Engineering Fundamentals*. Newnes.

Les Renardieres. 1981. “Negative discharges in long air gap at les Renardieres.” *Electra* 74:67–216.

March, Víctor, and Joan Montanyà. 2010. “Influence of the voltage-time derivative in X-ray emission from laboratory sparks.” *Geophys. Res. Lett.* 37:L19801. Accessed March 16, 2016. doi:10.1029/2010GL044543.

March, Víctor, and Joan Montanyà. 2011. “X-rays from laboratory sparks in air: The role of the cathode in the production of runaway electrons.” *Geophysical Research Letters* 38(4):L04803. Accessed March 16, 2016. doi:10.1029/2010GL046540.

March, Víctor, Joan Montanya, David Romero, Gloria Solà, and Oscar Van der Velde. 2012. “X-rays from laboratory sparks in air: The relationship between runaway electrons and the electric field.” Paper presented at the 31st International Conference on Lightning Protection (ICLP). Vienna, Austria, September 2-7.

March, Víctor. 2011. “X-ray emissions in high voltage impulses. Characterization of the runaway mechanism.” PhD diss. (in Spanish), Polytechnic University of Catalonia. BarcelonaTech.

Marx, Erwin O. 1924. “Versuche über die Prüfung von Isolatoren mit Spanningsstößen.” *Elektrotechnische Zeitschrift* 25:652–654.

Montanyà, Joan, Ferran Fabró, Oscar van der Velde, David Romero, Glòria Solà, Juan R. Hermoso, Serge Soula, Earle R. Williams, and Nicolau Pineda. 2014. *“*Registration of X-rays at 2500 m altitude in association with lightning flashes and thunderstorms.*” J. Geophys. Res. Atmos*. 119*:* 1492–1503.

Montanyà, Joan, Ferran Fabró, Víctir March, Oscar van der Velde, Glòria Sola, David Romero and Oriol Argemí. 2015b. “X-rays and microwave RF power from high voltage laboratory sparks.” *Journal of Atmospheric and Solar-Terrestrial Physics*. Accessed March 16, 2016. doi:10.1016/ j.jastp.2015.06.009.

Montanyà, Joan, Oscar van der Velde, and Earle R. Williams. 2015a. “The start of lightning: Evidence of bidirectional lightning initiation.” *Scientific Reports* 5:15180. Accessed March 16, 2016. doi:10.1038/srep15180.

Moore, Charles B., Kenneth B. Eack, Graydon D. Aulich, and William Rison, 2001: Energetic radiation associated with lightning stepped-leaders, *Geophys. Res. Lett.* 28:2141–2144.

Nguyen, Cung Vuong, Alexander P. J. van Deursen, and Ute Ebert. 2008. “Multiple x-ray bursts from long discharges in air.” *Journal of Physics D: Applied Physics* 41(23):234012. Accessed March 16, 2016. doi:10.1088/ 0022-3727/41/23/234012.

Nguyen, Cung Vuong, Alexander P. J. van Deursen, E. J. M. van Heesch, Hans G. J. J. Winands, and A J. M. Pemen, 2010. X-ray emission in streamer-corona plasma. *Journal of Physics D: Applied Physics* 43(2), 025202. Accessed March 16, 2016. doi:10.1088/0022-3727/43/2/025202.

Nguyen, Cung Vuong. 2012. “Experimental Study on Hard Radiation from Long Laboratory Spark Discharges in Air.” PhD diss., Eindhoven University of Technology.

Nijdam, Sander, E. Takahashi, Aram. H. Markosyan, and Ute Ebert. 2013. “Investigation of positive streamers by double pulse experiments, effects of repetition rate and gas mixture.” *Plasma Sources Science and Technology* 23(2):025008. Accessed March 16, 2016. doi: 10.1088/0963-0252/23/2/025008.

Nijdam, Sander, E. Takahashi, Jannis. Teunissen, and Ute Ebert. 2014. “Streamer discharges can move perpendicularly to the electric field.” *New Journal of Physics* 16(10):103038. Accessed March 16, 2016. doi:10.1088/1367-2630/16/10/103038.

Petersen, Danyal, and William Beasley. 2013. “Microwave radio emissions of negative cloud-to-ground lightning flashes.” *Atmos. Res.* Accessed March 16, 2016. doi:10.1016/ j.atmosres.2013.02.006.

Qin, Jianqi, and Victor P. Pasko. 2014. “On the propagation of streamers in electrical discharges.” *Journal of Physics D: Applied Physics* 47(43):435202. Accessed March 16, 2016. doi:10.1088/0022-3727/47/43/ 435202.

Rahman, Mahbubur, Vernon Cooray, Noor A. Ahmad, Johan Nyberg, Vladimir A. Rakov, and Sriram Sharma. 2008. “X rays from 80-cm long sparks in air.” *Geophysical Research Letters* 35(6):L06805. Accessed March 16, 2016. doi:10.1029/2007GL032678.

Rai, Jagdish, Rao Manoranjan and B. A. P. Tantry. 1972. “Bremsstrählung as a Possible Source of UHF Emissions from Lightning.” *Nature Physical Science* 238:59-60.

Rep’ev, A. G., and P. B. Repin. 2008. “Spatiotemporal parameters of the X-ray radiation from a diffuse atmospheric-pressure discharge.” *Technical Physics* 53(1):73–80. Accessed March 16, 2016. doi:10.1134/S106378420 8010143.

Rust, W. David, Paul R. Krehbiel, and A. Shalanta. 1979. “Measurements of radiation from lightning at 2200 MHz.” *Geophys. Res. Lett.* 6(2):85–8.

Stekolnikov, I. S., and A.V. Shkilev. 1962. “New information on the development of a negative spark and its comparison with lightning.” *Dokl. Akad. Nauk SSSR* 145:782–5.

Takagi, M., and T. Takeuti, 1963: Atmospheric radiation from lightning discharges, *Proc. Res. Inst. Atmos. Nagoya Univ*. 10:1–11.

van Deursen, Alexander P. J., and Pavlo O. Kochkin. 2015. “Some EMC aspects of a 2 MV marx generator with sensitive diagnostic equipment in the immediate vicinity.” Paper presented at the IEEE International Symposium on Electromagnetic Compatibility (EMC), Dresden, Germany, August 16-22.

Vayanganie, S. P. Amila, Vernon Cooray, Mahbubur Rahman, Pasan. Hettiarachchi, Oscar. Diaz, and M. Fernando. (2016). “On the occurrence of “bead lightning” phenomena in long laboratory sparks.” *Physics Letters A* 380(7-8):816–821. Accessed March 16, 2016. doi:10.1016/j.physleta. 2015.12.039.

Williams, Earle R. 2006. “Problems in lightning physics—The role of polarity asymmetry.” *Plasma Sources Sci. Technol.* 15:S91–S108.

Wilson, Charles Thomson R. 1925. “The electric field of a thundercloud and some of its effects.” *Proc. R. Soc. London* 37:32–37.

KD